Available online at www.sciencedirect.com

SCIENCE DIRECT®

Journal of Photochemistry and Photobiology A: Chemistry 181 (2006) 33–36

Journal of Photochemistry and Photobiology A:Chemistry

www.elsevier.com/locate/jphotochem

p-Type crystalline $HgCr_2S_4$ semiconductor electrode synthesis and its photoelectrochemical studies

V.V. Todkar[a], R.S. Mane[b], C.D. Lokhande[c], Sung-Hwan Han[b,*]

[a] Department of Chemistry, Bharati Vidyapeeth's College of Engineering for Women's, Katraj, Dhanakawadi, Pune 411043, India
[b] Department of Chemistry, Hanyang University, Sungdong-Ku, Haengdang-dong 17, Seoul 133-791, South Korea
[c] Thin Film Physics Laboratory, Department of Physics, Shivaji University, Kolhapur 416004, India

Received 21 July 2005; received in revised form 19 September 2005; accepted 23 October 2005

Abstract

A room temperature chemical synthesis of $HgCr_2S_4$ films has been carried out using controlled precipitation method. The films were polycrystalline and exhibited p-type electrical conductivity. $HgCr_2S_4$ films were found to be photoactive in KI solution. The PEC studies of these films have been carried out using *I–V*, output characteristics, spectral, speed, transient response and *C–V* characteristics.

Keywords: $HgCr_2S_4$; XRD; SEM; Photoelectrochemical properties

1. Introduction

It is noticed that there are very few p-type photocathodes such as $HgCr_2Se_4$, $CdCr_2Se_2$ and $CuInS_2$, $CuInSe_2$ [1–3] that have been reported as compared to the large number of n-type ferromagnetic spinel semiconductors (FSS) photoanodes for photoelectrochemical (PEC) cells [4,5]. $HgCr_2S_4$ is one of the important semiconductors with an insulating structure [6]. It shows anomalous optical effects with unusual magnetic behavior [7,8] attributed to the abnormal behavior of Hg. Recently, lot of attention has been received on this material due to its strong magneto-optical effects [9–11]. Due to simultaneous existence of ferromagnetism and semiconductivity in the same material offers many possibilities for novel devices and potential applications in a wide spectrum of electronics and optoelectronics [12–16]. Literature survey reveals that no p-type $HgCr_2S_4$ FSS film electrode has been reported till date in photoelectrode cell. Therefore, in this paper, we report the synthesis of p-type $HgCr_2S_4$ film electrode onto fluorine-doped-tin-oxide (FTO) substrates at ambient temperature. We studied PEC properties in potassium iodide electrolyte, which may enable capability of ambient temperature fabrication of p–n junction diode using a CdSe film for the n-layer.

2. Experimental

All AR grade (Aldrich) chemicals were used while $HgCr_2S_4$ film electrode synthesis. For the deposition of $HgCr_2S_4$ thin films, required amount of 0.1 M (10 mL) mercury chloride ($HgCl_2$) solution was mixed with 0.1 M (20 mL) chromic acid (CrO_3) solution in a glass beaker followed by 0.1 M (10 mL) disodium salt of ethylenediamine-tetraacetic acid (Na_2EDTA) solution. The pH of the bath ($\sim 10 \pm 0.2$) was kept constant by adding aqueous 25% ammonia solution. To this, under constant stirring, 0.1 M (30 mL) thiourea [$(NH_2)_2CS$] solution was added. The deposition was started by dipping the substrates (glass and FTO) in an alkaline bath maintained at 65 °C using controlled digital water bath for the period of 60 min. After the deposition, the substrates were taken out, rinsed with the double distilled water, dried and preserved in an airtight dark container.

Thickness of crystalline $HgCr_2S_4$ film electrode was measured by ellipsometry after standardization with Si single crystal using 630 nm monochromatic light source. As-deposited $HgCr_2S_4$ film electrode of thickness 314 nm was examined from X-ray diffraction pattern (XRD) recorded from Philips PW-1710 in the range of scanning angles 10–80° with Cu Kα radiation (1.5406 Å) and step size of 0.05°, and scanning electron microscopy (SEM) (JEOL JSI-220) for its crystal structure and surface morphology. For the PEC performance, $HgCr_2S_4$ film electrode onto FTO substrates was preferred. All photoelectro-

---

[*] Corresponding author. Tel.: +82 2 2292 5212; fax: +82 2 2290 0762.
E-mail address: shhan@hanyang.ac.kr (S.-H. Han).

1010-6030/$ – see front matter © 2005 Elsevier B.V. All rights reserved.
doi:10.1016/j.jphotochem.2005.10.024

chemical experiments were made using 1 M potassium iodide electrolyte, which is assumed to be an efficient hole scavenger. The distance between working electrode and counter electrode was 0.5 cm. Photocurrent–voltage curves were measured under 80 mW/cm^2 light illumination intensity. The spectral response of the PEC cell was recorded with monochromator in the wavelength range of 350–950 nm. The speed response of the cell was recorded as a rise and decay of photocurrent with time. Transient photoresponse of the cell was used to calculate decay constant. Capacitance–voltage (*C*–*V*) characteristics of the cell in terms of Mott–Schottky plot was used to determine the flat band potential (V_{fb}) of $HgCr_2S_4$ electrode using saturated calomel electrode (SCE) as a reference electrode.

3. Results and discussion

3.1. Crystal structure and surface morphology

Fig. 1 shows the X-ray powder diffraction pattern of the as-deposited film electrode onto glass substrate. The halo is due to the glass substrate. This halo peak position (15–35°) does not correspond to any peaks of the crystalline phase. XRD pattern shows remarkable textured growth structure along [2 2 0] direction, as evidenced by JCPDS data file card [27–0316] in addition to few other minor peaks viz. (3 1 1), (3 3 1), (4 2 2) and (5 1 1). There was good matching between observed, calculated, and standard interplanar spacing (*d*) values suggesting the formation of $HgCr_2S_4$. Fig. 2 shows the scanning electron micrograph (SEM) image of $HgCr_2S_4$ film electrode onto glass substrate. It is very easy to see under high magnification image, uniform grain growth with good film coverage. Interestingly, deep observation reveals well resolved, compact grains with irregular shape are aggregated to form homogeneous local edge-sharing network structure on substrate surface without void spaces. It shows a close packed structure with the average grain size falling in the nanometer range. Here, in support with reported phase, electron diffraction X-ray analysis, EDAX (inset of Fig. 1) linked with SEM unit, was carried out. The result is in agreement with that of XRD analysis (i.e. chemical compositional ratio, 1:2:4).

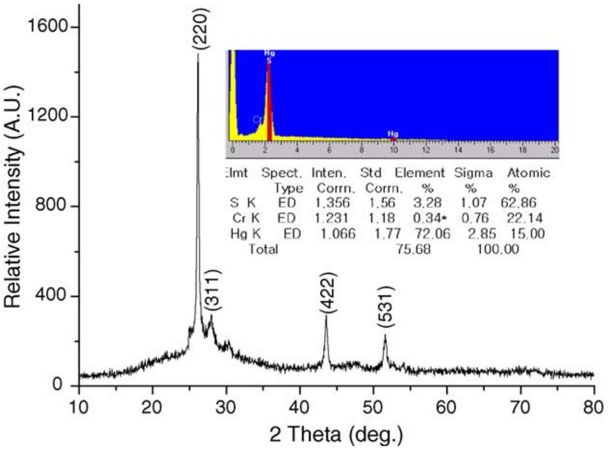

Elmt	Spect. Type	Inten. Corrn.	Std Corrn.	Element %	Sigma %	Atomic %
S K	ED	1.356	1.56	3.28	1.07	62.86
Cr K	ED	1.231	1.18	0.34*	0.76	22.14
Hg K	ED	1.066	1.77	72.06	2.85	15.00
Total				75.68		100.00

Fig. 1. X-ray diffraction pattern of 314 nm thick crystalline $HgCr_2S_4$ film. Inset shows good stoichiometric with chemical composition ratio 1:2:4.

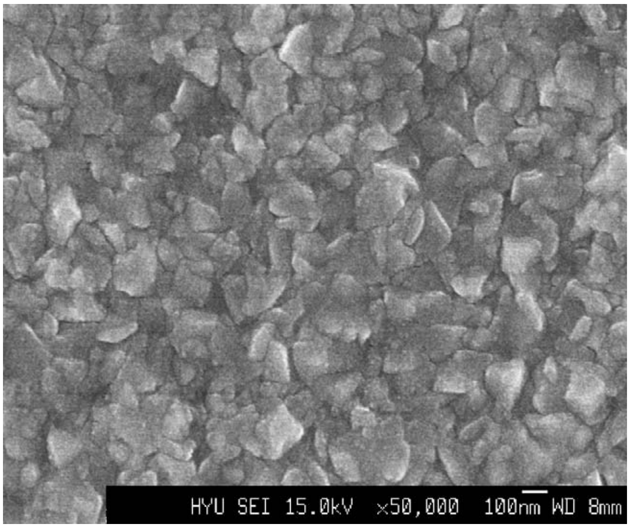

Fig. 2. SEM image of as-deposited crystalline $HgCr_2S_4$ film electrode onto glass substrate.

3.2. Conductivity type, I–V and output characteristics

PEC cell can be represented as $HgCr_2S_4$/polyiodiode electrolyte/graphite. It was observed that even when the external voltage is zero, the PEC cell in the dark exhibits some voltage, V_d and current, I_d. The polarity of the voltage is negative towards the $HgCr_2S_4$ electrode. The origin of this voltage is attributed to the difference between two half cell potentials in the PEC cell and can be written as:

$$E = E_{carbon} - E_{HgCr_2S_4} \quad (1)$$

where E_{carbon} and $E_{HgCr_2S_4}$ are the half-cell potentials when dipped in the potassium iodide electrolyte. From the above equation, one can write $E_{HgCr_2S_4} < E_{carbon}$.

Interestingly and as an expected, when above junction was illuminated by light of intensity 80 mW/cm^2, the magnitude of the voltage was changed from negative to positive towards the $HgCr_2S_4$ film electrode confirming p-type photoconducting performance. Current–voltage (*I*–*V*) characteristics of designed PEC cell with $HgCr_2S_4$ film electrode, under forward and reverse bias conditions in dark and under light illumination are shown in Fig. 3. The nature of the *I*–*V* curve indicates the formation of rectifying junction. In support to earlier conclusion, when the PEC cell was illuminated by light, the *I*–*V* curve was shifted in the second quadrant suggesting hole as a majority carriers and electron as a minority i.e. p-type behavior. Jundale et al. [17] showed same conducting behavior for p-Sm_2S_3 microcrystalline film electrode.

Increase in current under illumination indicates that $HgCr_2S_4$ films are photoactive. Using famous diode relation, junction ideality factor in dark and under light illumination were determined as 5.73 and 5.85, respectively. Increase in junction ideality factor under light illumination is attributed to average charge transfer across the semiconductor electrolyte with significant contribution from the surface states and deep traps [18,3]. The photovoltaic output curve was studied under light for understanding performance and device conversion efficiency (η%),

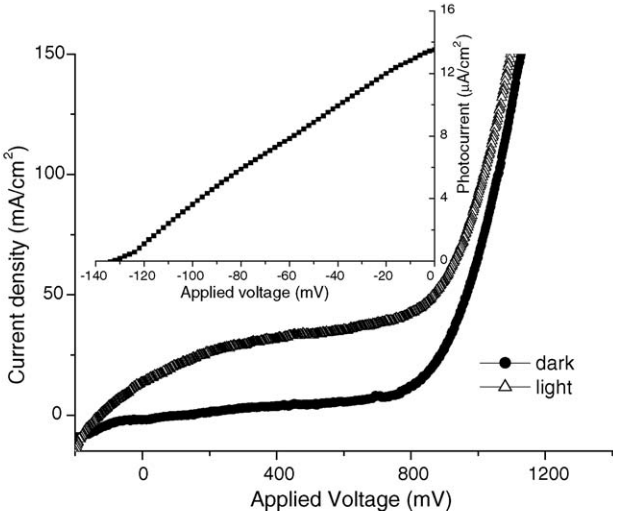

Fig. 3. (a) Current–voltage (*I*–*V*) characteristic in dark and under light illumination where, photocurrent enhancement in second quadrant confirming p-type performance of the cell is clearly seen with photovoltaic power output characteristics (inset).

which was calculated using $(I_{\max} \times V_{\max} \times A/P_{\mathrm{hv}}) \times 100\%$ equation, where P_{hv} is the power density of the incident radiation, A is the light collecting area (0.28 cm^2), $I_{\max}$ and $V_{\max}$ are, respectively, the current and voltage obtained at the maximum power point on the photovoltaic power output curve. For fill factor (FF) calculation, $(V_{\max} \times I_{\max}/V_{\mathrm{oc}} \times I_{\mathrm{sc}})$ relation was refereed with I_{sc} is the short circuit current and V_{oc} is the open circuit voltage. Series resistance, R_{s} and the shunt resistance, R_{sh} were evaluated from slopes of the power output curve [19]. Use of output characteristics (inset of Fig. 3) reveals 0.13% and 26% conversion efficiency and fill factor of the cell, respectively. The low efficiency in this investigation might be due to high series resistance (6600 Ω) and low value of shunt resistance (13.78 Ω) of the cell and interface states which are responsible for interactive recombination. It is interesting to note that the cell shows considerably high open circuit voltage (−135 mV, negative sign is due to its higher half cell potential), which in fact enthusiastic challenge to use effectively p–n junction heterojunction diode with other amorphous and/or crystalline n-type layer.

3.3. Spectral and speed response characteristics

Spectral response study of PEC cell can be described as a plot of photocurrent against wavelength (λ) for $HgCr_2S_4$ PEC cell is shown in Fig. 4. Using the plot, peak λ is obtained which estimates band gap energy 'E_g' (2.61 eV in the present case) of p-$HgCr_2S_4$ film electrode, which is in good agreement with reported elsewhere (2.60 eV) [14]. The decrease in photocurrent on longer and shorter wavelength sides is attributed to the transition between defect levels [20] and absorption of light in the electrolyte due to high surface recombination of photogenerated carriers by surface states [21], respectively. Speed response of PEC cell was measured as a plot of photocurrent as a time function (Fig. 5). It is noteworthy that rapid rise and fall (few microseconds) of current makes feasible to use this material as a light sensor.

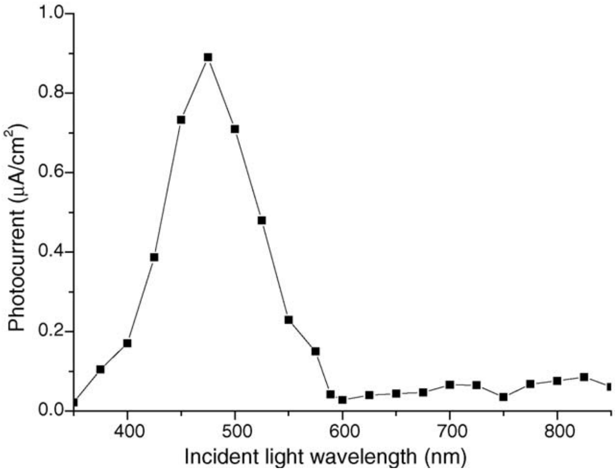

Fig. 4. Spectral response of FTO/$HgCr_2S_4$/polyiodide/graphite PEC cell.

3.4. Transient photoresponse and capacitance–voltage (*C*–*V*) characteristics

Transient photoresponse of PEC cell is the photovoltage rise and decay curve as shown in Fig. 6 reveals that increase in photovoltage is almost instantaneous. Interestingly, slow photovoltage decay which is uncommon in semiconducting thin films, as a function of time may be attributed to magneto-optical properties of ferromagnetic material [22,23] provides feature to see photoinduced magnetic storage properties [24]. Using the relation $V_{\mathrm{oc}}(t) = V_{\mathrm{oc}}(0) \times e^{-bt}$, where symbols have usual meanings, 3.45 'b' (decay constant) was calculated. Capacitance measurement as a function of applied voltage (*C*–*V*) (Fig. 7) gives useful information about photoelectrode such as type of conductivity, depletion layer width and flat band potential, V_{fb}. V_{fb} is an important factor in explaining charge transfer processes across the semiconductor–electrolyte junction and estimated from Mott–Schottky relation by standardizing with saturated

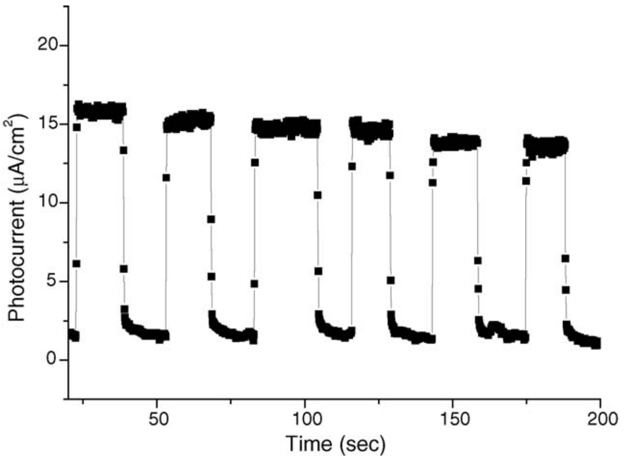

Fig. 5. Rise and decay of photocurrent as a function of time, where instantaneous performance was recorded enable to use electrode as light sensor.

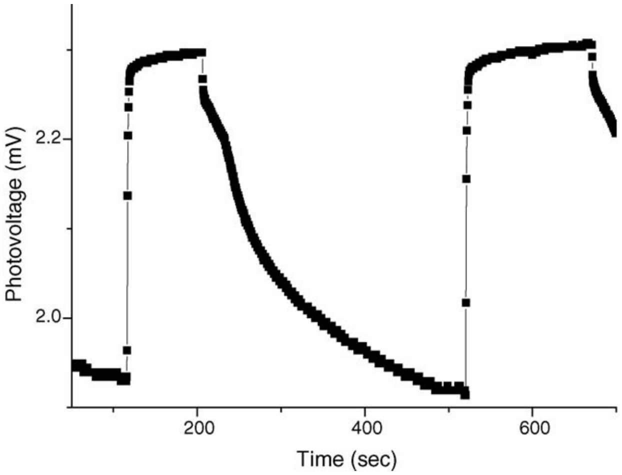

Fig. 6. Photoinduced open circuit voltage (V_{oc}) as a time function, which was further used (decay part) for decay constant measurement.

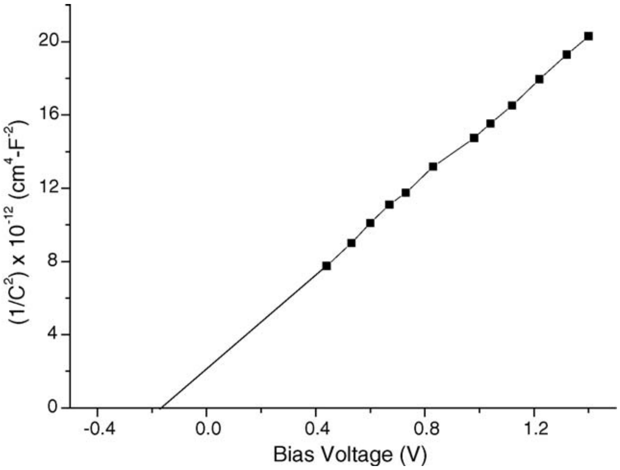

Fig. 7. Mott–Schottky plot of above formed PEC cell for estimating flat band potential, V_{fb}.

calomel electrode (SCE). The variation of $1/C^2$ versus electrode potential (V) is non-linear as seen in Fig. 7, which is an indication of graded junction formation between $HgCr_2S_4$ and potassium iodide electrolyte. Non-planar interfaces, surface roughness, presence of stacking faults due to irregular and sharp surface morphology, ionic adsorption on the film electrode surface may be the possible reasons for the deviation from linearity in C–V plot. The value of the flat band potential was obtained by extrapolating the straight line portion to the zero value and was found to be −0.14 V (SCE) for $HgCr_2S_4$–potassium iodide redox electrolyte, which is a measure of electrode potential at which band bending is zero.

4. Conclusions

In conclusion, a simple chemical deposition method has been used for the crystalline growth of stoichiometric p-type $HgCr_2S_4$ film electrode consisting irregular and compact grains, since the primary cause is the lack of a p-type crystalline ferromagnetic semiconductor because the p–n junction is the origin of various active functions of semiconductors onto FTO coated glass substrates from an aqueous alkaline bath (pH ∼ 10) at ambient temperature. X-ray diffraction measurement confirmed the crystalline quality of as-grown film electrode with cubic structure and preferential orientation along (0 0 2) plane. The PEC properties were studied in potassium iodide electrolyte. Nevertheless, this chemical method shows promise as a low cost for the preparation of p-type electrodes as essential for device fabrication.

Acknowledgments

One of the authors, RSM would like to thank Brain Korea 21 (BK-21) project and National R and D project for Nano-Science and Technology, Korea for the award of POST-DOC research fellowship. This work has been carried out with financial support from the ABRL R14-2003-014-01001-0.

References

[1] G.K. Padam, Mater. Res. Bull. 22 (1987) 789.
[2] R.S. Becker, G.D. Zhou, J. Elton, Solar Energy Mater. 12 (1985) 371.
[3] H.J. Lewerenz, H. Goslowsky, F. Thiel, Solar Energy Mater. 9 (1983) 159.
[4] D.S. Sutrave, G.S. Shahane, J.S. Dargad, L.P. Deshmukh, Ind. J. Pure Appl. Phys. 34 (1996) 506.
[5] A.M. Salem, M.E. El-Ghazzawi, Semicond. Sci. Technol. 19 (2004) 236.
[6] M. Jelonek, A. Winiarski, A. Chelkowski, Phys. Status Solidi A 57 (1980) K5.
[7] G. Harbeke, S.B. Berger, F.P. Emmenegger, Solid State Commun. 6 (1968) 553.
[8] P.K. Baltzer, P.J. Wojtowicz, M. Robbins, E. Lopatin, Phys. Rev. 151 (1966) 367.
[9] R.S. Mane, B.R. Sankpal, K.M. Gadve, C.D. Lokhande, Mater. Res. Bull. 34 (1999) 2035.
[10] J.K. Furdyno, J. Appl. Phys. 53 (1982) 7637.
[11] S.J. Lade, R.S. Mane, M.D. Uplane, C.D. Lokhande, Trans. SAEST 32 (1997) 72.
[12] P. Hoschl, P. Hlidek, V. Kubla, P. Moravec, J. Pitel, V. Prosser, J. Crystal Growth 52 (1981) 669.
[13] M.N. Spallart, G. Tamizhmani, C.L. Clement, J. Electrochem. Soc. 137 (1990) 3434.
[14] S. Faria, US Patent Specification 4,374,917 (to GET Products Corporation) (1983).
[15] A.K. Sood, K. Wu, J.N. Zemel, Thin Solid Films 48 (1978) 73.
[16] L.A. Rodriguez, S. Gordillo, Solar Energy Mater. 19 (1989) 421.
[17] S.B. Jundale, C.D. Lokhande, Solar Energy Mater. Sol. Cells 28 (1992) 151.
[18] A. Chemseddine, R. Morineau, J. Lirage, Solid State Ionics 9 (1983) 357.
[19] T.J. Coutes, Solar Energy Mater. 50 (1978) 99.
[20] R.S. Mane, B.R. Sankpal, C.D. Lokhande, Thin Solid Films 353 (1999) 29.
[21] K.M. Gadave, C.D. Lokhande, Ind. Pure Appl. Phys. 31 (1993) 942.
[22] L.L. Golik, S.M. Grigorovitch, M.I. Elinson, Z.E. Kunkova, Y.M. Ukrainskyi, Thin Solid Films 34 (1976) 279.
[23] S.S. Unterricker, I. Burlakov, F. Schneider, M. Dietrich, V. Tsurkan, I.M. Tiginyand, The ISOLDE Collaboration, J. Phys. Chem. Sol. 64 (2003) 2069.
[24] A. Dei, Angew. Chem. Int. Ed. 44 (2005) 1160.